Catalytic hydrogenation of n-butene with nanosized Pt/NBCNT hybrid membranes reinforced with bacterial cellulose

Bilal El Mrabate, Ádám Prekob, László Vanyorek, Emília Csiszár, Ferenc Kristály, Máté Leskó & Zoltán Németh

Springer

Springer

Catalytic hydrogenation of *n*-butene with nanosized Pt/NBCNT hybrid membranes reinforced with bacterial cellulose

Bilal El Mrabate[1,2], Ádám Prekob[1,2], László Vanyorek[1,2], Emília Csiszár[3], Ferenc Kristály[4], Máté Leskó[4], and Zoltán Németh[1,2,*]

[1] Higher Education and Industry Cooperation Centre of Advanced Materials and Intelligent Technologies, University of Miskolc, Miskolc 3515, Hungary

[2] Institute of Chemistry, University of Miskolc, Miskolc 3515, Hungary

[3] Department of Physical Chemistry and Materials Science, Budapest University of Technology and Economics, Műegyetem rkp. 3, Budapest 1111, Hungary

[4] Institute of Mineralogy and Geology, University of Miskolc, Miskolc 3515, Hungary

ABSTRACT

One of the main challenges in the field of heterogeneous catalysis is the involvement of thin solid films and membranes and their application in flow systems. In this regard, we report here the application of self-supported bacterial cellulose (BC) reinforced nanosized platinum (Pt)/N-doped bamboo-like carbon nanotube (NBCNT) hybrid catalyst membrane with a thickness of 35 ± 5 μm in the hydrogenation of *n*-butene. To synthetized the BC-NBCNT/Pt nanohybrid membrane catalyst a simple impregnation route was applied in a two-step process. As-prepared material was tested in a continuous flow system and the conversion was followed directly by using Fourier transform infrared spectroscopy. Furthermore, the fabricated films were characterized by scanning electron microscopy, X-ray diffraction, energy-dispersive X-ray spectroscopy and specific surface area measurement (Brunauer–Emmett–Teller). Hydrogenation performance was studied on both single and double films. Results revealed that 97% conversion of *n*-butene can be achieved using these bacterial cellulose reinforced hybrid membranes.

GRAPHIC ABSTRACT
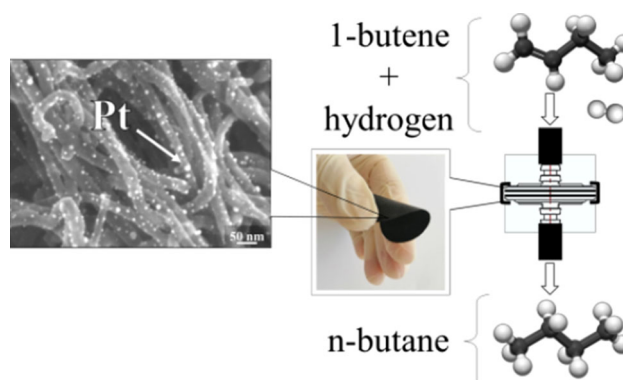
Introduction

There has been growing interest over the last decade in the involvement of hybrid materials in the field of catalysis, due to advantages such as high specific surface area, simplicity of operation or high material conversion efficiency [1]. As the expectations for hybrid and composite structures are increasing continuously, research is focusing on the design of catalysts combining nanomaterials and metallic particles.

Among transition metals, platinum (Pt) and Pt-based materials are regarded as highly active and effective catalysts [2]. It is well known that nanosized Pt has one of the highest catalytic activity levels in chemical reactions [3] and catalytic hydrogenation [4] due to its high active surface area [5]. Consequently, Pt-based catalysts should be ultrafine powders containing Pt particles in the nanometre range to offer a large number of active sites and a large surface area. However, the work with ultrafine powder used in hydrogenation treatments in gas or liquid state often possesses technical challenges. To overcome limitations and to further improve the effectiveness of catalysts, many researchers have focused on the development of material-supported Pt catalysts. In this regard, carbon nanotubes (CNTs) [6] and bacterial cellulose (BC) [7] are of interest in the development of a novel hybrid membrane catalyst for a wide range of applications.

CNTs, especially multi-walled carbon nanotubes (MWCNTs) and N-doped bamboo-shaped carbon nanotubes (NBCNTs), are often used as promising support material to stabilize Pt nanoparticles and are applied in catalytic reactions such as hydrocarbon oxidation [8] or hydrogenation reactions [9] owing to their high specific surface area [10] and excellent thermal conductivity parameters [11]. Using fibrous cellulose as a support of the carbon nanotubes, membrane layer can be formed, which provides longer and more efficient contact between the catalytic nanoparticles and gas molecules. Furthermore, both the cellulose fibres and carbon nanotubes are lack of microporosity, which causes the formation of metal nanoparticles on the easily accessible binding sites, providing higher mass transfer on the surface. In our previous works, precious metal contained catalysts in different forms was tested. NBCNT supported Pt catalysts and Pt contained NBCNT coated zeolite beads was examined in the hydrogenation of 1-butene [12] and Pd contained carbonized ion exchange resin beads were also tested [13]. It was proven that they are efficient, but higher amount of catalysts is required to reach high catalytic efficiency.

When applying NBCNT as a support material, the interaction between the Pt nanoparticles and the surface of carbon nanotubes can be increased. Further adsorption sites appear due to the incorporated nitrogen atoms, which increase the potential interactions with the catalytically active metals and leads to

the formation of more effective heterogeneous catalysts [14].

Nowadays, bacterial cellulose (BC) has attracted rapidly growing worldwide scientific interest, in which particular attention has been paid to BC-based advanced functional materials [15]. Furthermore, their nanofibrillar structure and high mechanical strength offer tremendous potential applications in various fields, such as the application of hybrid membrane technology in catalysis [16]. Basically, two routes allow in situ generation of nanoparticles, either by taking advantage of the chemical stability of BC towards the reducing agent or by using the reducer property of BC towards a metal salt [15]. This latter case represents a more innovative route, relying on the reducing and coordinating behaviour of BC, as shown by other types of cellulose that lead to metal salt reduction and the formation of Pt [17]. BC-supported nanoparticles performance in catalytic hydrogenation [18] or hydrogen evolution [19] reactions have been investigated recently. Furthermore, Yang et al. [20] developed alternative new hydrocarbon-based polymer membranes applying a Pt decorated BC electrode.

The preparation of Pt nanoparticles using fibrous materials—e.g. BC and CNT—could be one of the most promising ways for hybrid membrane catalyst development, since these materials form 3D networks which allow the deposition of Pt nanoparticles on their surface cavities [7]. As the poor conductivity of BC can hinder its application as a support of the catalyst, the development of hybrid membranes could be an alternative way to improve the catalytic properties of as-prepared materials. One option is using CNTs, which have the highest conductivity among carbon materials [21]. Although a recent review presents the advantages and usage of cellulose, nanocellulose and carbon nanotubes mixed materials [22], the preparation and application of BC-supported CNT membranes deposited with Pt nanoparticles still have not investigated widely. Aritonang et al. [7] presented two different synthesis routes for the deposition of Pt particles on the BC-MWCNT hybrid membrane surfaces. The BC was immersed either in a solution of Pt precursors ($PtCl_4$ and H_2PtCl_6) or in surfactant stabilized MWCNT suspension. While both of the applied synthesis techniques provided Pt particles on the surface of membranes, their average particle size differed: it was 26 nm and 42 nm, respectively.

To improve the drawbacks (e.g. rather large particle size of Pt) of these methods, the main objective of this study is to prepare a novel BC-supported hybrid membrane catalyst applying NBCNT and Pt nanoparticles with an average particle size under 5 nm and to explore its application in the catalytic hydrogenation of n-butene.

Experimental section

Materials

N-doped BCNTs was produced by the chemical vapour deposition (CVD) method following our previous work [23]. In brief, nickel (II) nitrate hexahydrate (Merck) and magnesium oxide (Merck) were used as the catalyst and n-butylamine was applied as the carbon source (Sigma-Aldrich) in a tube furnace at 700 °C in nitrogen flow. To remove the residual support material and catalytic particles, the as-prepared N-doped BCNTs were treated with cc. hydrochloric acid (36 wt%) under vigorous stirring for 2 h, then washed with distilled water. BC fibres were received from nata de coco cubes (FI, Philippines) by alkaline and oxidative purification and mechanical disintegration [24]. For catalytically active hybrid membrane preparation, an aqueous suspension of BC and BCNT with a dry solid content of 1% and hexachloroplatinic (IV) acid was used. Nitrogen (99.995%, Messer) and hydrogen (99.999%, Messer) were used for activation of the membrane catalyst. Catalytic tests were carried out by hydrogenation of 1-butene (99.500%, Messer). A polytetrafluoroethylene (PTFE) filter of the pore size of 0.22 μm and the diameter of 47 mm (Durapore-GVWP04700) was used for membrane production.

Membrane preparation

To prepare the BC-NBCNT/Pt nanohybrid membranes, the calculated amount of BC fibres was dipped into 15 cm^3 EtOH. Meanwhile, the NBCNT was sonicated in 50 cm^3 EtOH for 15 min. The content of the NBCNT in the final nanohybrid membrane was 90 w/w%. Then, the BC suspension was added to the NBCNT suspensions and the mixture was stirred for 5 h at 300 rpm. Finally, the preparation of BC-based hybrid membranes was accomplished by vacuum filtration through a PTFE membrane to achieve a

loading of 8.0 ± 0.9 mg/cm^2 (total mass 100 ± 10 mg/membrane), then each membrane was dried in air.

In the next step, as-prepared BC-NBCNT membranes (100 mg) were impregnated by a 0.5 cm^3 20 wt% platinum solution (0.04 g H$_2$PtCl$_6$ $\times$ H$_2$O in 0.5 cm^3 water). Two similar synthesis routes were published recently [7]. During the process, 0.25 cm^3 of platinum solution was added dropwise to both sides of the membranes. Impregnated membranes were dried at 120 °C overnight. Finally, BC-NBCNT/Pt membranes were hydrogenated at 400 °C for 30 min in a tube furnace with a hydrogen flow rate of 50 mL/min.

Characterization

The surface morphology of BC-NBCNT/Pt hybrid membranes was verified by scanning electron microscopy (SEM). SEM measurements were done with Thermo Helios G4 PFIB CXe and JEOL JSM 7200F instruments. Energy-dispersive X-ray spectroscopy (EDAX) measurement was completed by a scanning electron microscope (Thermo Helios G4 PFIB CXe) and an Ametek EDAX Octane Elect Plus (detector area 30 mm^2) device.

The presence and physiognomy of platinum nanoparticles on the surface of hybrid membranes were investigated by X-ray diffraction (XRD), with a Bruker D8 Advance diffractometer (Cu-Kα source, 40 kV and 40 mA generator settings), equipped with a Vantec1 position sensitive detector (1 window opening). The parallel beam geometry of the instrument (by Göbel mirror) allowed measurements to be made at the milligram level, without the need for pressing powder specimens. Zero background sample holders (Si crystal cut) eliminated the issue of sample transparency, thus no sample holder contribution presents. Measurements were taken in the 2°–100° (2θ) range with 0.007° (2θ)/14 s goniometer speed, on top-loaded specimens in zero background Si sample holders.

The hydrogenation process of 1-butene and the catalytic activity of the BC-NBCNT/Pt membranes was followed by vertex 70 type Fourier transform infrared spectroscope (FTIR) in a gas cell with a KBr window.

A nitrogen (N$_2$) adsorption–desorption experiment was performed at 77 K to determine the surface area and micropore volume (t-plot method) using ASAP
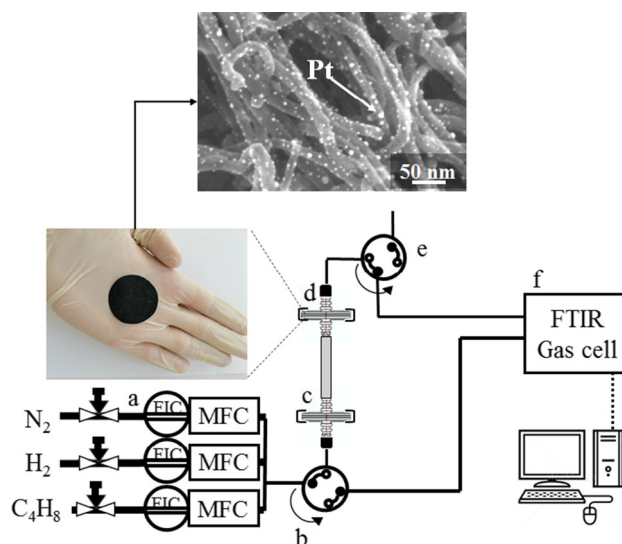

Figure 1 Experimental setup of catalytic hydrogenation of 1-butene. **a** Values for the gases (N$_2$, H$_2$, C$_4$H$_8$), **b**, **e** four-way valve for gas inlet into the reactor and the FTIR gas cell, **c**, **d** membrane holders, **f** FTIR instrument connected to a computer.

2020 sorptometer, (Micromeritics Instrument Corp Germany). Prior to each measurement, the samples were degassed at 90 °C for 24 h.

To determine the catalytic activity of the BC-NBCNT/Pt hybrid membranes, 1-butene hydrogenation was tested in a continuous flow system (Fig. 1), which is coupled to the gas cell of the FTIR equipment [13].

Before the experiments, the FTIR instrument was calibrated by the usage of an H$_2$/N$_2$/1-butene gas mixture applying four different 1-butene concentrations at room temperature and atmospheric pressure. For each measurement, two hybrid membranes with a weight of 100 mg were used. The flow rates of the applied gases were 40 mL/min (N$_2$, H$_2$) and 20 mL/min (1-butene) at atmospheric pressure. The reaction temperature was set at 50 °C and the molar ratio of the hydrogen to 1-butene was 2:1. The catalytic performance of BC-NBCNT/Pt hybrid membranes was determined by the conversion ($X\%$) of 1-butene using the equation below (Eq. 1):

$$X\%_{1-\text{butene}} = \frac{\text{consumed } n_{1-\text{butene}}}{\text{initial } n_{1-\text{butene}}} \times 100. \qquad (1)$$

Figure 2 SEM images (**a–c**), bright-field (**d**) and high-angle annular dark-field (**e**) STEM images, XRD pattern (**f**), EDS spectrum (**g**) and particle size distribution (**h**) of the Pt/NBCNTs-cellulose membrane.
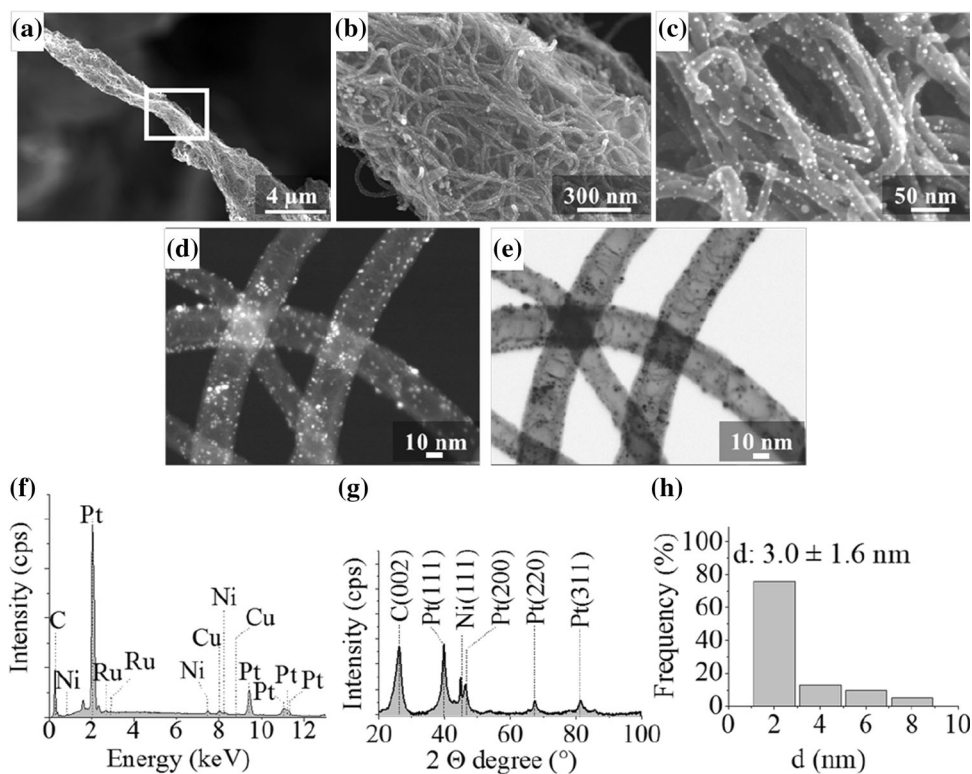
Results and discussion

Characterization of the BC-NBCNT/Pt hybrid membranes

The BC-reinforced NBCNT/Pt membranes were examined by scanning electron microscopy. The SEM image of the membrane shows the fibrous structure of the NBCNTs and BC fibres (Fig. 2a). The formation of the fibre bundles is explained by interactions between the surface functional groups of BC and NBCNTs [25]. The oxygen contained functional groups—hydroxyl groups—of the NBCNTs and BC was able to form hydrogen bonds, which provided for the adsorption of NBCNTs on the surface of the BC fibres. The nitrogen doped carbon nanotubes contain several incorporated nitrogen atoms which contributed to anchoring on the cellulose surface. At higher resolution (Fig. 2b, c), the Pt nanoparticles are visible in homogenous distribution on the nanotube surface, which thoroughly examined by bright-field and high-angle annular dark-field imaging in STEM mode (Fig. 2d, e). The presence of NBCNT and BC did not affect the average particle sizes of Pt nanoparticles during the nanocomposite fabrication procedure and aggregation or bigger particles could

not be observed in the structure of hybrid membranes. The presence of elemental platinum on the membrane surface was confirmed by XRD measurements. On the diffractograms, the visible peaks belong to the reflexions of the Pt (111), Pt (200), Pt (220) and Pt (311); these are found at 39.9°; 46.6°; 67.6°; 81.3° two Theta angles, respectively (Fig. 2f). The presence of the Ni (111) reflexion is explained by the catalyst remaining after the NBCNT synthesis. A small amount of nickel nanoparticles was enclosed in the structure of the NBCNTs and could not be removed. The carbon layers of NBCNTs prevented the dissolution of nickel in hydrochloric acid during the purification step. The C (002) peak confirms the presence of carbon nanotubes. The bands of platinum, nickel and carbon were also located on the EDS spectrum (Fig. 2g). In case of the platinum nanoparticles, high dispersion was detected: the measured average diameter was 3.0 ± 1.6 nm (Fig. 2h). The vast majority of the nanoparticles, namely 95%, were smaller than 3.3 nm, the smallest diameter was 1.8 nm, but a few nanoparticles had a size between 8 and 10 nm. This particle distribution approximates a homo-dispersal system. Based on these results, we can conclude that applying the BC-NBCNT support allowed the formation of the small particles.
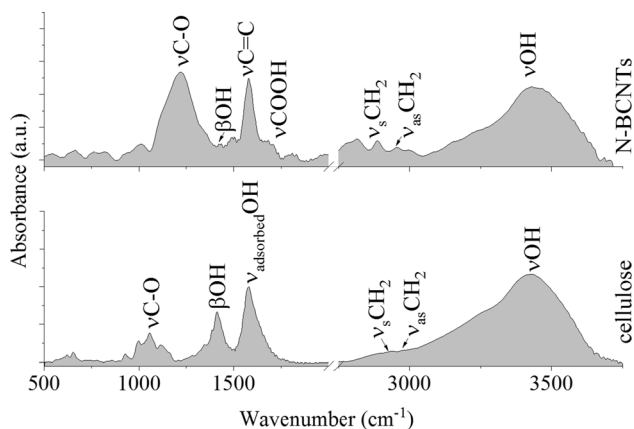
Figure 3 FTIR spectrum of the nanocrystalline cellulose fibres and the NBCNTs.

Table 1 Summary of BET surface area values of raw materials and BC-NBCNT/Pt membranes

Sample name	BET surface area (m^2/g)
NBCNT	146
BC	1
BC-NBCNT/Pt	110
BC-NBCNT/Pt (used 1)	107
BC-NBCNT/Pt (used 2)	109

The surface functional groups of the BC and NBCNTs were identified by FTIR spectroscopy (Fig. 3). Vibration bands of the C–O stretching are found on the spectrums at 1223 cm^{-1} (NBCNTs) and at 1059 cm^{-1} (BC). Bending vibration of the hydroxyl groups results in a peak at 1431 cm^{-1} in the case of NBCNTs and at 1413 cm^{-1} on the spectrum of BC. The adsorption peak at 1574 cm^{-1} can be attributed to the C=C bands on the spectra of NBCNTs, which corresponds to the vibration of the lattice structure of the NBCNTs. The peak located at 1590 cm^{-1} belongs to the vibration mode of water molecules absorbed in BC [26]. At the 1713 cm^{-1} wavenumber, the band corresponds to the carboxyl (COOH) groups on the NBCNTs. The peaks around 2889 cm^{-1} and 2952 cm^{-1} are attributed to the symmetric and asymmetric C–H stretching vibration. The intensive peak at 3455 cm^{-1} on the spectrum of NBCNTs belongs to the –OH stretching vibration. The band at 3414 cm^{-1} in case of cellulose is characteristic of the stretching vibration of the hydroxyl group in polysaccharides, furthermore it also includes the inter- and intra-molecular hydrogen bond vibrations in BC [27, 28]. Several –OH groups are found on the NBCNTs and BC fibres which could make interactions and lead to the formation of hydrogen bridges. These facilitates formed the fibres into bundles, as seen in the SEM image (Fig. 2a). A further advantage of the functional groups containing oxygen is that they may regulate the particle size of catalytically active metals during catalyst preparation. Moreover, the ion-binding effect of the oxygen-containing groups (electric interaction, ion exchange and surface complexation interactions) should not be forgotten.

The as-prepared NBCNT-based membranes were also characterized by N_2 adsorption technique to measure their specific surface area. The BET surface area values of raw materials and hybrid membranes can be seen in Table 1. It can be concluded that the addition of support material slightly reduces the surface area from 146 to 110 m^2/g. However, significant difference in the surface area values measured before and after the catalytic reaction cannot be measured.

Catalytic test of the Pt/NBCNT-cellulose membranes: hydrogenation of 1-butene

For the confirmation of the BC-NBCNT/Pt membrane catalyst applicability, an easily followable gas phased reaction was chosen, which is the most widely used method in catalytic research for fast testing of catalysts. The hydrogenation of 1-butene was carried out in a continuous flow system by the application of two membranes. The weight hourly space velocity (WHSV) was 27.45 kg 1-butene/1 kg catalyst/1 h. The 1-butene concentration was checked in a hydrogen–nitrogen gas mixture by FTIR measurements. The 1-butene concentration was calculated based on the change of the C=C vibration
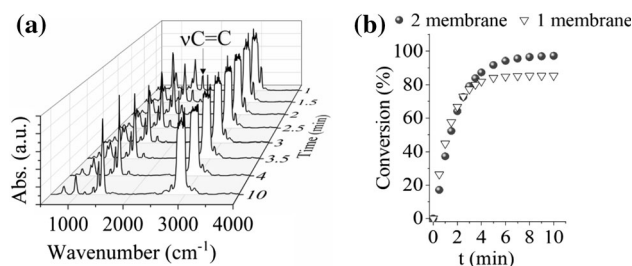

Figure 4 FTIR spectrums of the 1-butene-hydrogen-nitrogen-butane mixture versus time of hydrogenation (**a**); 1-butene conversion verses hydrogenation time by applying of 1 or 2 membranes (**b**).

band intensity at 1646 cm^{-1} wavenumber (Fig. 4a); this measuring mode was calibrated with different amounts of olefin containing N$_2$–H$_2$ mixtures. By applying only one of the two membranes, the yielded 1-butene conversion was 85.3% and after 7 min the membrane catalyst reached its maximum catalytic activity (Fig. 4b). By using two membranes, the 1-butene conversion improved to 98% by 10 min hydrogenation. The membranes are very thin (35 ± 5 µm); nonetheless, they are catalytically efficient for hydrogenation for olefin in a gas phase reaction. Their remarkable catalytic behaviour can be explained by the very high dispersibility of platinum nanoparticles ($d_{av} = 3.0$ nm) and the homogenous coverage per Pt particle of the fibres in the membrane matrix.

Conclusion

Bacterial cellulose combined with a nitrogen doped bamboo-like carbon nanotube support membrane was prepared with a thickness of 35 ± 5 µm. The membrane was impregnated by hexachloroplatinic acid, after reduction in the hydrogen flow, which resulted in a very efficient Pt hybrid membrane catalyst. The platinum nanoparticles homogenously covered the surface of the nanofibres in the membrane. The particle sizes are exceptionally small and the 3.0 ± 1.5 nm average diameter led to richly coated nanotube surfaces in the self-supporting membrane. The particle size of platinum is almost homogeneously dispersed, 95% of the particle diameters were between 1.8 and 3.3 nm, owing to the presence of oxygen-containing functional groups on the fibres. As the multiple SEM analysis demonstrated, the morphology of the membranes was uniform, indicating that the preparation of membranes was reproducible by following our well-designed and appropriate methodology.

One of the major disadvantages of conventionally used catalysts forms (e.g. beads) is that the gases can bypass the catalyst particles, thereby decreasing the conversion efficiency. This obstacle can be avoided by the application of membrane catalyst because the molecules of gases diffuse through the pores of membrane (formed by Pt-coated fibres), providing a better contact between the catalytically active phase and the reactant molecules. Other advantage of this hybrid membrane is that it contains –OH groups on

the surface of fibres, which promotes the adsorption of platinum ions. Additionally, the Pt nanoparticles were efficiently dispersed on the surface of the fibres leading to a homogenous coverage of nanotubes and carbon fibres by the catalytically active phases. The uniformly located Pt particles facilitate the encounters of molecules on the surface of catalyst. The BC-NBCNT support membrane is applicable for the deposition of highly dispersive platinum nanoparticles on its surface, opening new pathways for the application of hybrid membrane technology. Owing to the interactions between the surface functional groups (–OH, –COOH) of nanotubes and cellulose, bundles were formed, which built up the membrane structure. The platinum decorated self-supporting nanofibred membranes were tested in gas-phased hydrogenation of 1-butene in continuous flow system. By using two membranes, high 1-butene conversion (98%) was reached after 10 min with continuous flow.

Compliance with Ethical Standards

Conflict of interest On behalf of all authors, the corresponding author states that there is no conflict of interest.

References

[1] Ye R, Zhao J, Wickemeyer BB et al (2018) Foundations and strategies of the construction of hybrid catalysts for optimized performances. Nat Catal 1:318–325

[2] Lim DH, Lee WD, Lee HI (2008) Highly dispersed and nano-sized Pt-based electrocatalysts for low-temperature fuel cells. Catal Surv Asia 12:310–325. https://doi.org/10.1007/s10563-008-9059-z

[3] Ozturk Z, Sen F, Sen S, Gokagac G (2012) The preparation and characterization of nano-sized Pt-Pd/C catalysts and comparison of their superior catalytic activities for methanol and ethanol oxidation. J Mater Sci 47:8134–8144. https://doi.org/10.1007/s10853-012-6709-3

[4] Li X, Li G, Zang W et al (2014) Catalytic activity of shaped platinum nanoparticles for hydrogenation: a kinetic study. Catal Sci Technol 4:3290–3297. https://doi.org/10.1039/c4cy00580e

[5] Bergamaski K, Pinheiro ALN, Teixeira-Neto E, Nart FC (2006) Nanoparticle size effects on methanol electrochemical oxidation on carbon supported platinum catalysts. J Phys Chem B 110:19271–19279. https://doi.org/10.1021/jp063337h

[6] Liu X, Villacorta R, Adame A, Kannan AM (2011) Comparison of Pt/MWCNTs nanocatalysts synthesis processes for proton exchange membrane fuel cells. Int J Hydrog Energy 36:10877–10883. https://doi.org/10.1016/j.ijhydene.2011.05.141

[7] Aritonang HF, Onggo D, Ciptati, Radiman CL (2015) Insertion of platinum particles in bacterial cellulose membranes from PtCl4 and H2PtCl6 Precursors. In: Macromolecular symposia. Wiley-VCH Verlag, pp 55–61

[8] Xiong H, Wiebenga MH, Carrillo C et al (2018) Design considerations for low-temperature hydrocarbon oxidation reactions on Pd based catalysts. Appl Catal B Environ 236:436–444. https://doi.org/10.1016/j.apcatb.2018.05.049

[9] Sikora E, Prekob Á, Halasi G et al (2018) Development and application of carbon-layer-stabilized, nitrogen-doped, bamboo-like carbon nanotube catalysts in Co2 hydrogenation. ChemistryOpen 7:789–796. https://doi.org/10.1002/open.201800162

[10] Peigney A, Laurent C, Flahaut E et al (2001) Specific surface area of carbon nanotubes and bundles of carbon nanotubes. Carbon N Y 39:507–514. https://doi.org/10.1016/S0008-6223(00)00155-X

[11] Han Z, Fina A (2011) Thermal conductivity of carbon nanotubes and their polymer nanocomposites: a review. Prog Polym Sci 36:914–944

[12] Vanyorek L, Prekob Á, Baráth M et al (2019) Development of nitrogen-doped bamboo-like carbon nanotubes coated zeolite beads as "support on support" catalyst for the catalytic hydrogenation of olefins. React Kinet Mech Catal 127:705–714. https://doi.org/10.1007/s11144-019-01592-y

[13] Prekob Á, Hajdu V, Muránszky G et al (2020) Application of carbonized ion exchange resin beads as catalyst support for gas phase hydrogenation processes. React Kinet Mech Catal 129:85–94. https://doi.org/10.1007/s11144-019-01694-7

[14] Li YH, Hung TH, Chen CW (2009) A first-principles study of nitrogen- and boron-assisted platinum adsorption on carbon nanotubes. Carbon N Y 47:850–855. https://doi.org/10.1016/j.carbon.2008.11.048

[15] Foresti ML, Vázquez A, Boury B (2017) Applications of bacterial cellulose as precursor of carbon and composites with metal oxide, metal sulfide and metal nanoparticles: a review of recent advances. Carbohydr Polym 157:447–467

[16] Wang J, Tavakoli J, Tang Y (2019) Bacterial cellulose production, properties and applications with different culture methods: a review. Carbohydr Polym 219:63–76

[17] Johnson L, Thielemans W, Walsh DA (2011) Synthesis of carbon-supported Pt nanoparticle electrocatalysts using nanocrystalline cellulose as reducing agent. Green Chem 13:1686–1693. https://doi.org/10.1039/c0gc00881h

[18] Chen M, Kang H, Gong Y et al (2015) Bacterial cellulose supported gold nanoparticles with excellent catalytic properties. ACS Appl Mater Interfaces 7:21717–21726. https://doi.org/10.1021/acsami.5b07150

[19] Mi Y, Wen L, Wang Z et al (2016) Ultra-low mass loading of platinum nanoparticles on bacterial cellulose derived carbon nanofibers for efficient hydrogen evolution. Catal Today 262:141–145. https://doi.org/10.1016/j.cattod.2015.08.019

[20] Yang J, Sun D, Li J et al (2009) In situ deposition of platinum nanoparticles on bacterial cellulose membranes and evaluation of PEM fuel cell performance. Electrochim Acta 54:6300–6305. https://doi.org/10.1016/j.electacta.2009.05.073

[21] Li W, Liang C, Zhou W et al (2003) Preparation and characterization of multiwalled carbon nanotube-supported platinum for cathode catalysts of direct methanol fuel cells. J Phys Chem B 107:6292–6299. https://doi.org/10.1021/jp022505c

[22] Miyashiro D, Hamano R, Umemura K (2020) A review of applications using mixed materials of cellulose, nanocellulose and carbon nanotubes. Nanomaterials 10:186–208

[23] Vanyorek L, Muranszky G, Sikora E et al (2018) Synthesis optimization and characterization of nitrogen-doped bamboo-shaped carbon nanotubes. J Nanosci Nanotechnol 19:429–435. https://doi.org/10.1166/jnn.2019.15776

[24] Gea S, Reynolds CT, Roohpour N et al (2011) Investigation into the structural, morphological, mechanical and thermal behaviour of bacterial cellulose after a two-step purification process. Bioresour Technol 102:9105–9110. https://doi.org/10.1016/j.biortech.2011.04.077

[25] Qi H, Liu J, Mäder E (2014) Smart cellulose fibers coated with carbon nanotube networks. Fibers 2:295–307. https://doi.org/10.3390/fib2040295

[26] Poletto M, Pistor V, Zeni M, Zattera AJ (2011) Crystalline properties and decomposition kinetics of cellulose fibers in wood pulp obtained by two pulping processes. Polym Degrad Stab 96:679–685. https://doi.org/10.1016/j.polymdegradstab.2010.12.007

[27] Popescu MC, Popescu CM, Lisa G, Sakata Y (2011) Evaluation of morphological and chemical aspects of different wood species by spectroscopy and thermal methods. J Mol Struct 988:65–72. https://doi.org/10.1016/j.molstruc.2010.12.004

[28] Fackler K, Stevanic JS, Ters T et al (2011) FT-IR imaging microscopy to localise and characterise simultaneous and selective white-rot decay within spruce wood cells. Holzforschung 65:411–420. https://doi.org/10.1515/HF.2011.048